AGU PUBLICATIONS

Tectonics

RESEARCH ARTICLE
10.1002/2014TC003748

**Key Points:**
- Sanya of Hainan Island, China was linked with Western Australia in the Cambrian
- Sanya had not juxtaposed with South China until the Ordovician
- Gondwana terminally suture along the southern margin of South China

**Supporting Information:**
- Readme
- Figure S1
- Figure S2
- Table S1
- Table S2

**Correspondence to:**
Y. Du,
duyuansheng126@126.com

**Citation:**
Xu, Y., P. A. Cawood, Y. Du, Z. Zhong, and N. C. Hughes (2014), Terminal suturing of Gondwana along the southern margin of South China Craton: Evidence from detrital zircon U-Pb ages and Hf isotopes in Cambrian and Ordovician strata, Hainan Island, *Tectonics*, *33*, 2490–2504, doi:10.1002/2014TC003748.

Received 29 SEP 2014
Accepted 20 NOV 2014
Accepted article online 25 NOV 2014
Published online 18 DEC 2014

# Terminal suturing of Gondwana along the southern margin of South China Craton: Evidence from detrital zircon U-Pb ages and Hf isotopes in Cambrian and Ordovician strata, Hainan Island

**Yajun Xu[1,2,3], Peter A. Cawood[3,4], Yuansheng Du[1,2], Zengqiu Zhong[2], and Nigel C. Hughes[5]**

[1]State Key Laboratory of Biogeology and Environmental Geology, School of Earth Sciences, China University of Geosciences, Wuhan, China, [2]State Key Laboratory of Geological Processes and Mineral Resources, School of Earth Sciences, China University of Geosciences, Wuhan, China, [3]Department of Earth Sciences, University of St. Andrews, St. Andrews, UK, [4]Centre for Exploration Targeting, School of Earth and Environment, University of Western Australia, Crawley, Western Australia, Australia, [5]Department of Earth Sciences, University of California, Riverside, California, USA

**Abstract** Hainan Island, located near the southern end of mainland South China, consists of the Qiongzhong Block to the north and the Sanya Block to the south. In the Cambrian, these blocks were separated by an intervening ocean. U-Pb ages and Hf isotope compositions of detrital zircons from the Cambrian succession in the Sanya Block suggest that the unit contains detritus derived from late Paleoproterozoic and Mesoproterozoic units along the western margin of the West Australia Craton (e.g., Northampton Complex) or the Albany-Fraser-Wilkes orogen, which separates the West Australia and Mawson cratons. Thus, in the Cambrian the Sanya Block was not part of the South China Craton but rather part of the West Australian Craton and its environs. In contrast, overlying Late Ordovician strata display evidence for input of detritus from the Qiongzhong Block, which constituted part of the southeastern convergent plate margin of the South China Craton in the early Paleozoic. The evolving provenance record of the Cambrian and Ordovician strata suggests that the juxtaposition of South China and West Australian cratons occurred during the early to mid-Ordovician. The event was linked with the northern continuation of Kuungan Orogeny, with South China providing a record of final assembly of Gondwana.

## 1. Introduction

Assembly of the disparate blocks of Gondwana (Figure 1) commenced in the Neoproterozoic but was not complete until the Cambrian [*Meert*, 2003; *Collins and Pisarevsky* 2005; *Cawood and Buchan*, 2007; *Boger*, 2011]. Two of the major collisional belts related to Gondwana formation are the East African-Antarctic Orogen [*Grunow et al*., 1996; *Jacobs et al*., 1998; *Meert and Van der Voo*, 1997; *Zhao et al*., 2002] and the Kuungan Orogen (also known as the Pinjarra Orogen) [*Meert et al*., 1995; *Meert and Van der Voo*, 1997; *Fitzsimons*, 2000a, 2000b; *Boger et al*., 2001; *Meert and Lieberman*, 2008]. The former marks the Mozambique suture (550–520 Ma) between the blocks of west Gondwana (African, South America) and the Indian and Antarctic cratons, whereas the latter defines the Kuunga suture (530–490 Ma) between the West Gondwana-Indo-Antarctic and Australia-Antarctic cratons (Figure 1) and is considered to mark the site of final assembly of Gondwana [e.g., *Meert*, 2003; Boger, 2011]. Within Antarctica, the Kuunga suture passed through Prydz Bay and trends southward into the interior of the continent along three proposed routes (Figure 1) [*Fitzsimons*, 2000a; *Boger et al*., 2001; *Meert*, 2003; *Boger and Miller*, 2004; *Liu et al*., 2007a, 2007b]. Its continuation to the north of Prydz Bay is mostly unconstrained, in part due to the loss of the early Paleozoic northern margin of east Gondwana through the combined effects of subduction of Greater India under Asia and Cenozoic deformational overprint on the surviving segments from this collision event [*Yin*, 2006; *Gehrels et al*., 2011; *Smit et al*., 2014]. Timing of final Gondwana assembly was synchronous with the development of an unconformity between Cambrian and Ordovician strata along the northern margin of east Gondwana that extends from North India to Western Australia and also occurs in displaced Gondwana fragments in Southeast Asia [*Cawood and Nemchin*, 2000; *Collins*, 2003; *Gehrels et al*., 2006a, 2006b; *Cawood et al*., 2007; *Myrow et al*., 2010; *Zhu et al*., 2011; *Metcalfe*, 2013; *Zhao et al*., 2014]. Uplift and erosion associated with the formation of the unconformity surface were also associated with

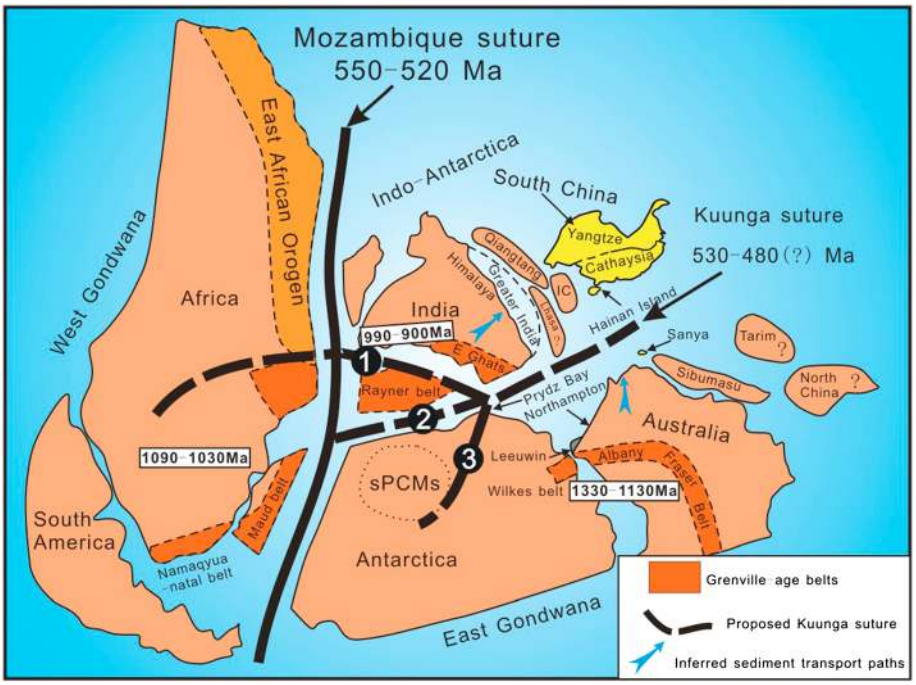


**Figure 1.** Simplified reconstruction of Gondwana showing the location of South China and three proposed routes of the Kuunga suture [modified from *Boger et al*., 2001] and its northward continuation (this study). The configuration of other blocks and continents considered synthetically those of *Cocks and Torsvik* [2013], *Usuki et al*. [2013], *Metcalfe* [2013], and *Ali et al*. [2013]. (1) Position of Kuunga suture proposed by *Meert* [2003]. (2) Position of Kuunga suture proposed by *Boger and Miller* [2004]. (3) Position of Kuunga suture proposed by *Fitzsimons* [2003]. sPCMs = southern Prince Charles Mountains. IC = Indochina.

penetrative deformation, metamorphism, and igneous activity [*DeCelles et al*., 2000; *Gehrels et al*., 2003; *Cawood et al*., 2007; *Chatterjee et al*., 2007; *Yin et al*., 2010a, 2010b; *Myrow et al*., 2010; *Wang et al*., 2013a], which *Cawood et al*. [2007] referred to as the Bhimphedian Orogeny.

Geochemical, provenance, and paleontological data suggest that during the Neoproterozoic and Paleozoic, South China lay along the northern margin of Gondwana (Figure 1) [*Zhao and Cawood*, 1999, 2012; *Jiang et al*., 2003; *Hughes et al*., 2005; *Hofmann et al*., 2011; *Cawood et al*., 2013;] and was covered by sediments sourced from the adjoining segments of east Gondwana [*Yu et al*., 2008; *Wang et al*., 2010; *McKenzie et al*., 2011a; *Xu et al*., 2013, 2014]. It likely represents a distal fragment of Greater India lithosphere [*Cawood et al*., 2013; *Xu et al*., 2013, 2014]. The sedimentary break between Cambrian and Ordovician strata that is recognized along the margin of northeast Gondwana is present in the southern part of South China at Yunkai and on Hainan Island (Figure 2) [*Bureau of Geology and Mineral Resources of Guangdong Province* (*BGMRGP*), 1988; *Wang et al*., 2007]. At Yunkai, the base of the Ordovician strata contains clasts inferred to be derived from late Neoproterozoic basement of the Himalaya region and from the recycling of underlying Cambrian strata [*Xu et al*., 2014]. On Hainan Island, there is an unconformity between Cambrian and Ordovician strata [*BGMRGP*, 1988] and in this paper we outline the provenance record of these units to further track the development and character of the early Paleozoic orogenic event. Our data provide further constraint on the disposition of blocks along the northern margin of Gondwana near the extension of the Kuunga suture.

## 2. Geological Setting

The South China Craton consists of the Yangtze Block to the northwest and the Cathaysia Block to the southeast (Figure 2). Each includes Archean and Paleoproterozoic basement units that were assembled and accreted along the margin of Rodinia via a series of early to mid-Neoproterozoic accretionary arc complexes

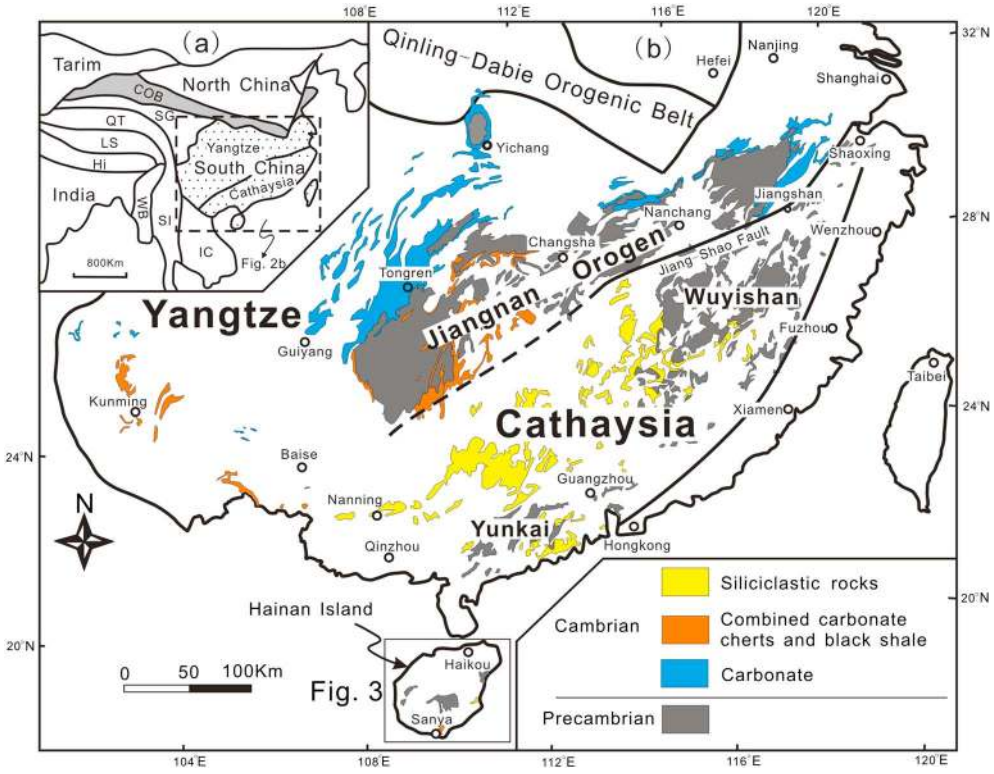


**Figure 2.** (a) Tectonic outline of East Eurasia [modified from *Metcalfe*, 2006] and (b) simplified geological map of the South China Craton showing the main tectonostratigraphic units and the Cambrian sequence [modified from *Xu et al*., 2013]. Abbreviations in Figure 2a: COB = Central Orogenic Belt of China, SG = Songpan-Ganze Accretionary Complex, QT = Qiangtang Block, LS = Lhasa terrane, Hi = Himalaya terrane, SI = Sibumasu Block, WB = West Burma terrane, and IC = Indochina Block.

[*Zhao and Cawood*, 1999, 2012; *Zhou et al*., 2002; *Zhao et al*., 2011; *Cawood et al*., 2013; *Wang et al*., 2013b; *Y. J. Wang et al*., 2014].

Hainan Island is located off the southern coast of South China and is separated from the mainland by the Qiongzhou Strait (Figures 2b and 3). Late Paleozoic to Mesozoic granitoids dominate exposures on the island, with Proterozoic, Paleozoic, Mesozoic, and Cenozoic rocks preserved in isolated outcrops (Figure 3).

The Proterozoic Baoban and Shilu groups (~ 1800–1400 Ma) [*Ma et al*., 1997; *Li et al*., 2002, 2008; *Zhao and Guo*, 2012] constitute basement and are exposed on the western part of the island, south of Changjiang. The amphibolite facies Baoban Group consists of gneisses and schists, intruded by granodiorites dated at 1431 ± 5 Ma and 1436 ± 7 Ma [*Li et al*., 2002]. The greenschist facies Shilu Group is composed of metavolcanic rocks that have yielded U-Pb zircon ages of 1433 ± 6 Ma and 1439 ± 9 Ma [*Li et al*., 2008] and iron-rich metasedimentary rocks. The unconformably overlying Shihuiding Formation is composed of quartzite and quartz schists with a maximum depositional age of 1200 Ma, based on the age of the youngest detrital zircon grain [*Li et al*., 2008].

Contrasting early Paleozoic successions are exposed at Wanning and Sanya (Figure 3) that constitute separate lithotectonic successions that we refer to as the Qiongzhong and Sanya blocks, respectively [*Yang et al*., 1989]. Outcrop of both successions is poor due to the thick vegetation and agricultural activity in the tropical humid environment on the island. Strata in the Qiongzhong Block include early Cambrian neritic clastic rocks with carbonates at the top of succession. Contact relations with adjoining units are not preserved. The age is constrained on the basis of the microfossils *Siphogonuchites triangulates* Qian and *Lapworthella* sp., which occur in the carbonates [*Zhang and Jiang*, 1998], and both the overall lithology and fossil assemblage are similar to time equivalent strata on the mainland of South China [*BGMRGP*, 1988; *Zhang and Jiang*, 1998; *Yao et al*., 1999]. The Ordovician succession in the center of the island at Tunchang

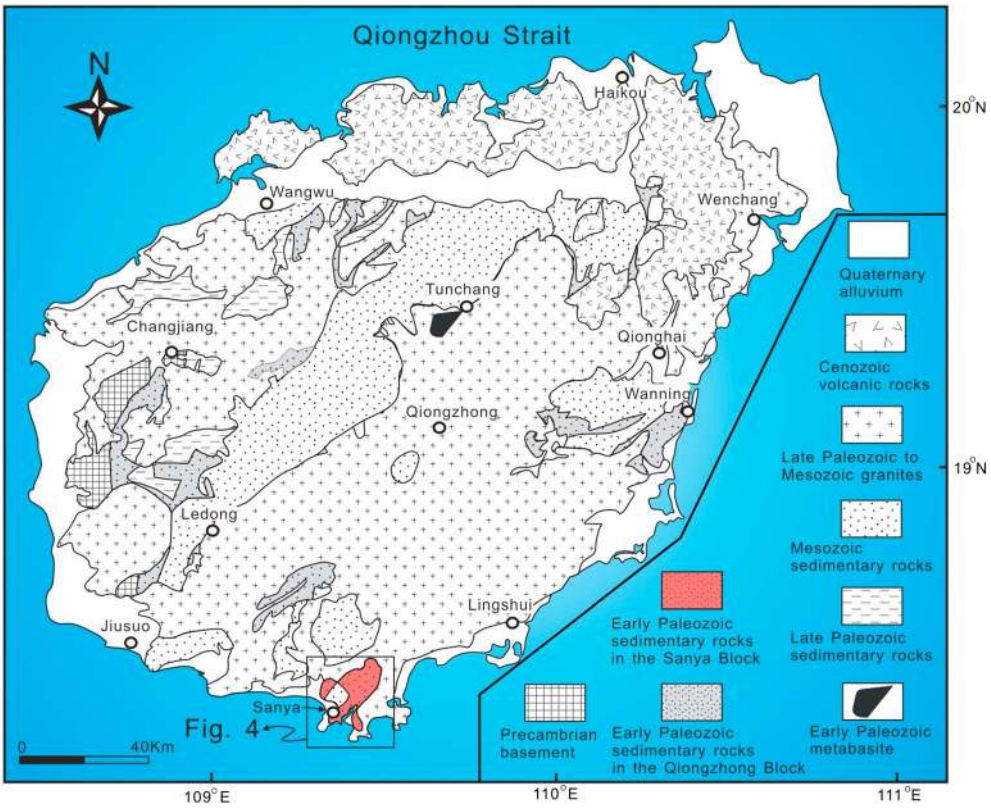


**Figure 3.** Simplified geological map of Hainan Island showing the main tectonostratigraphic units and the study area.

is composed of low-grade metasedimentary, basic volcanic, and volcaniclastic rocks that are in turn conformably overlain by a Silurian succession of neritic sandstones [*BGMRGP*, 1988; *Xu et al*., 2007]. At Sanya (Figure 3), the Cambrian succession is composed of quartz sandstone, calcareous argillite, siltstone, and manganese and phosphate-bearing carbonates [*BGMRGP*, 1988; *Xu et al*., 2007]. It contains middle Cambrian trilobite genera *Xystridura* and *Galahetes* [*Sun*, 1963; *Zhu and Lin*, 1978; *Li and Jago*, 1993]. The sedimentary and fossil assemblages are comparable with those in the Australia and are distinct from those on the mainland of South China [*Sun*, 1963; *BGMRGP*, 1988; *Zeng et al*., 1992; *Zhang and Jiang*, 1998]. These units are unconformably overlain by Ordovician to Silurian conglomerates, sandstones, siltstones, and intercalated carbonates [*Wang et al*., 1991; *Zeng et al*., 1992; *Xu et al*., 2007]. The early Paleozoic successions at Wanning and Sanya are unconformably overlain by Upper Devonian to Permian quartzite, conglomerate, diamictite shale, and limestone, which are in turn unconformably overlain by Mesozoic and Tertiary siliciclastic strata [*BGMRGP*, 1988; *Wang et al*., 1991].

Intrusive and extrusive igneous rocks are widespread across Hainan Island (Figure 3). Middle Permian to Middle Triassic (~ 270–230 Ma) [*Li et al*., 2006; *Xie et al*., 2006] and Cretaceous granites (~ 130–90 Ma) [*Wang et al*., 1991] constitute more than 60% of the island's area. Cenozoic basalts crop out across the northern part of the island.

The distinctive early Paleozoic successions in the Qiongzhong and Sanya blocks have been referred to as separate tectonostratigraphic terranes, but due to the isolated nature of successions, the position and orientation of the boundary is unresolved [*Yang et al*., 1989; *Xia et al*., 1991; *Metcalfe*, 1996].

## 3. Stratigraphy and Sampling

This study is focused on the Cambrian strata of the Sanya Block and overlying Ordovician strata (Figure 4). The base of the succession is the lower Cambrian Mengyueling Formation, which is conformably overlain by the middle Cambrian Damao Formation [*BGMRGP*, 1988]. Both consist of interstratified quartz sandstone

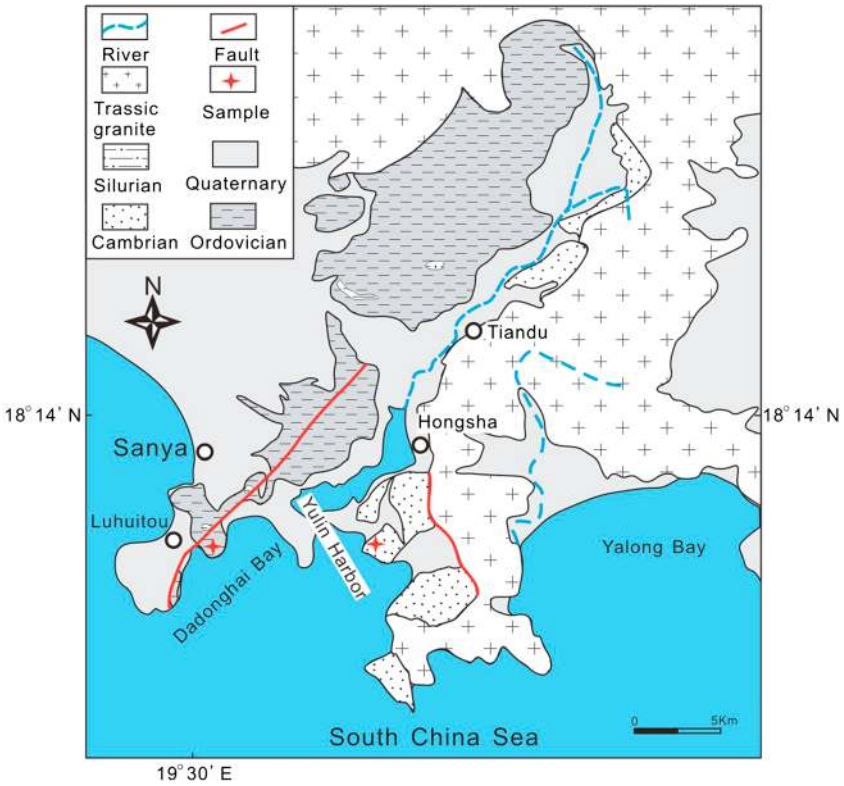


**Figure 4.** Simplified geological map of the Sanya area showing the location of analyzed samples.

and mudstone with the younger unit including manganese and phosphate-bearing carbonates and cherts toward the top. The Cambrian succession is overlain unconformably by the Ordovician Dakui, Yahua, Shatang, Yuhong, Jianling, and Gangoucun formations. These are an interstratified, conformable succession of conglomerate, quartz sandstone, mudstone, and carbonate. The lower Silurian Kongliecun Formation is in fault contact with the older rock units.

Three samples were collected for LA-ICPMS U-Pb dating and Hf isotope analysis of detrital zircons; two (11SY-1 and 11SY-2) from the Damao Formation along the eastern side of Yulin Harbor and one (12LHT-2) from the Shatang Formation on the western side of the harbor (Figure 4). Samples 11SY-1 and 11SY-2 are cream, well-sorted, medium-grained quartz sandstones, containing more than 95% quartz and minor lithic fragments. Sample 12LHT-2 is a pale black siltstone. Representative photomicrographs of each sample are presented in Figure S1 in the supporting information.

## 4. Analytical Methods

Zircons were separated by conventional heavy liquid and magnetic techniques. A random selection of grains were mounted in epoxy resin, sectioned approximately in half, and polished. All analyses were conducted at the State Key Laboratory of Geological Processes and Mineral Resources, China University of Geosciences in Wuhan. Cathodoluminescence (CL) imaging was conducted to assess the internal structure of grains. Zircon U-Pb dating was undertaken on an Agilent 7500a laser ablation inductively coupled plasma mass spectrometer (LA-ICP-MS) using an excimer laser ablation system (GeoLas 2005). All measurements were normalized relative to standard zircons 91500 and GJ-1. Detailed operating conditions and data reduction are outlined by *Liu et al*. [2010]. Common Pb correction was not performed as the measured $^{204}$Pb signal is low and U-Pb ages are concordant or nearly concordant. Concordia diagrams, histograms, and probability distribution plots were made using Isoplot/Ex_ver3 [*Ludwig*, 2003]. Excel program "Age pick," from the University of Arizona, USA, was used to calculate age peaks that include at least three analyses [*Gehrels et al*., 2011].

Zircon Hf isotope analysis was carried out in situ using a Neptune Multicollector-ICP-MS in combination with a Geolas 2005 excimer ArF laser ablation system. Instrumental conditions and data acquisition follow *Hu et al*. [2012]. Analyses were conducted with a beam diameter of 44 μm and a hit rate of 6 Hz. Analytical spots were located close to, or on the top of, LA-ICP-MS spots, or in the same growth domain as inferred from CL images. Reference zircons 91500 and GJ-1 were used to monitor accuracy of the interference correction during Hf analysis. Zircon 91500 yielded a $^{176}Hf/^{177}Hf$ ratio 0.282303 ± 8 ($n$ = 20, 1$\sigma$) compared to the recommended value of 0.282308 ± 6 [*Blichert-Toft*, 2008] and 0.282008 ± 6 ($n$ = 8, 1$\sigma$) for GJ-1 compared to the recommended value of 0.282015 ± 19 [*Elhlou et al*., 2006].

The $\varepsilon_{Hf}(t)$ values were calculated relative to the chondritic reservoir with a $^{176}Hf/^{177}Hf$ ratio of 0.282772 and $^{176}Lu/^{177}Hf$ of 0.0332 [*Blichert-Toft and Albarede*, 1997]. The decay constant for $^{176}Lu$ of 1.867 × 10–11a-1 was adopted [*Soderlund et al*., 2004]. Single-stage Hf model ages ($T_{DM}$) were calculated by reference to depleted mantle with a present-day $^{176}Hf/^{177}Hf$ ratio of 0.28325 and $^{176}Lu/^{177}Hf$ ratio of 0.0384 [*Vervoort and Blichert-Toft*, 1999]. Two-stage Hf model ages ($T_{DM2}$) were calculated by assuming a mean $^{176}Hf/^{177}Hf$ value of 0.015 for the average continental crust [*Griffin et al*., 2002]. The single-stage Hf model ages ($T_{DM}$) were taken for grains derived from juvenile magma generated directly from the depleted mantle or by remelting of material recently extracted from depleted mantle. They have $\varepsilon_{Hf}(t) \geq 0.75$ times the $\varepsilon_{Hf}$ values of the depleted mantle curve. The two-stage Hf model ages ($T_{DM2}$) were calculated for all other analyses and are inferred to be generated by reworking of older crust with addition of juvenile material [*Belousova et al*., 2010].

## 5. Results

### 5.1. Detrital Zircon U-Pb Ages

A total of 222 analyses were undertaken on 222 zircon grains. Cathodoluminescence (CL) images of representative zircons are presented in Figure S2 in the supporting information. Zircon U-Pb isotopic compositions are presented in Table S1. Uncertainties on individual analyses in the data table and concordia plots are presented at 1$\sigma$. Concordia plots as well as histograms and frequency plots, which are based on analyses with greater than 90% concordancy, for the samples are shown in Figure 5.

#### 5.1.1. Cambrian Sandstone Samples (11SY-1 and 11SY-2)

Zircons from the Cambrian samples are subhedral or rounded crystals, generally 260 to 360 μm in length. Most grains display oscillatory zoning in CL images and a few show homogeneous structures. No core-rim structures were observed (Figures S2a and S2b).

One hundred thirty analyses were conducted on 130 zircon grains from samples 11SY-1 and 11SY-2, and yielded 122 concordant ages of which 111 zircons show oscillatory zoning and have Th/U ratios of 0.2–1.9, suggesting a magmatic origin. The remaining 11 concordant grains display a homogeneous internal structure and are interpreted as metamorphic in origin (Figure S2b), although they have Th/U ratios varying in the range of 0.2–0.5. Age spectra for the two samples show a similar range of ages as well as a similar distribution of age frequencies (Figures 5d and 5e). Crystallization ages of magmatic zircons are mainly grouped in the age range from 1700 Ma to 900 Ma. Sample 11SY-1 has a principal age peak at 1266 Ma ($n$ = 38) (Figure 5d). Sample 11SY-2 has a single main peak at 1111 Ma ($n$ = 36) (Figure 5e). Combining the data from the two samples yielded a combined single peak at 1142 Ma ($n$ = 69) (Figure 6b). Two analyses in sample 11SY-1 yielded older ages of 2633 ± 49 Ma and 2244 ± 38 Ma. Ages of metamorphic zircons lie in the range 1550–1640 Ma, 1130–1270 Ma, and 1010–1090 Ma.

#### 5.1.2. Ordovician Sandstone Sample (12LHT-2)

Zircons from the Ordovician sample are generally 120 to 300 μm in length and display a euhedral to subhedral morphology. Most grains show oscillatory zoning and a few display homogeneous structures in CL images. A small number of grains are enveloped by narrow rims (Figures S2c and S2d).

Ninety-eight zircon spots were analyzed in the core region of 98 grains and generated 92 concordant ages (Figure 5c). They include 90 crystallization ages on magmatic zircons showing oscillatory zoning (Figure S2c) with Th/U ratios of 0.2–3.2, whereas two grains of inferred metamorphic origin display a homogeneous structure (Figure S2d) and have Th/U ratios of 0.3 and 0.53. Most of the magmatic zircon ages lie in the ranges of 1940–910 Ma (77 grains, 85% of population) and 520–450 Ma (7 grains, 8% of population), with age peaks at 1727 Ma ($n$ = 19), 1521 Ma ($n$ = 26), 1400 Ma ($n$ = 21), 1225 Ma ($n$ = 15),

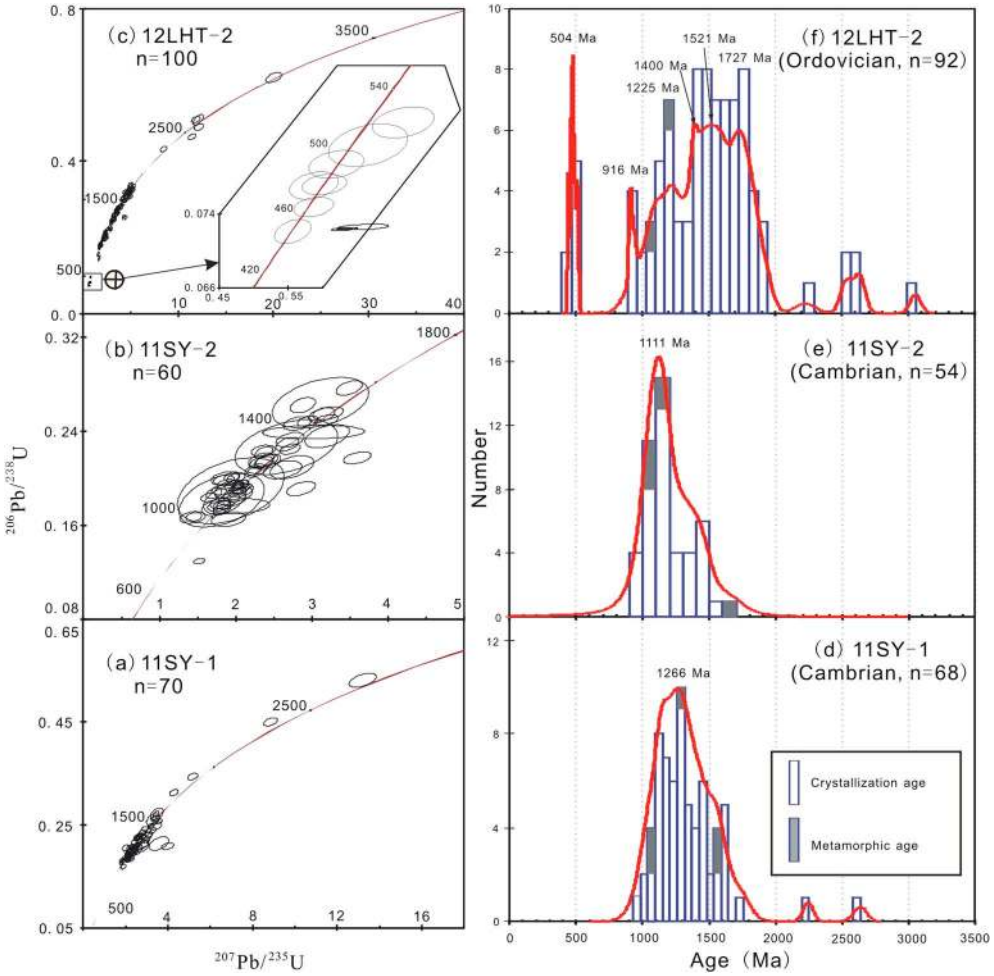


**Figure 5.** Concordia plots for the two sandstones from (a and b) the Cambrian and one siltstone from (c) the Ordovician and (d–f) their relative probability density diagram of ages with concordance of between 90% and 110%; *n* = number of analyses, Ages less than 1000 Ma are based on the $^{206}Pb/^{238}U$ ratio, whereas older ages are based on the $^{207}Pb/^{206}Pb$ ratio.

916 Ma ($n = 7$), and 504 Ma ($n = 3$). One analysis yielded an age of ~ 2220 Ma. Four analyses occur in the range of 2600–2500 Ma. The oldest age is 3053 ± 40 Ma. The two metamorphic ages are 1043 ± 57 Ma and 1192 ± 100 Ma (Figure 5f).

### 5.2. Zircon Hf Isotope Compositions

Zircons Hf isotope analyses were conducted on 30 zircons from Cambrian sample 11SY-1 with U-Pb ages of 1.3–1.0 Ga and from 68 grains from Ordovician sample 12LHT-2 covering a range of U-Pb ages (3000–450 Ma). Variations in Hf isotope ratios $\varepsilon_{Hf}(t)$ with their U-Pb ages ($t$) are plotted in Figure 6. Detailed Hf isotope compositions are presented in Table S2 in the supporting information.

Zircons with ages of 1.3–1.0 Ga from 11SY-1 exhibit $\varepsilon_{Hf}(t)$ values of +0.3 to +12.5 and with Hf model ages ranging from 1.9 Ga to 1.2 Ga (Figure 6a). Most of them are derived from reworking of older crust with significant additions of juvenile materials. Eight grains have $\varepsilon_{Hf}(t)$ values $\geq 0.75$ that of the Depleted Mantle indicating derivation largely from juvenile material.

Zircons from 12LHT-2, with crystallization ages of 3.0–0.9 Ga, exhibit a large range of $\varepsilon_{Hf}(t)$ values from −21.2 to 17.3 and model ages from 3.2 Ga to 1.2 Ga, even within single U-Pb age populations. They are inferred to be derived from the reworking of older crustal components with additions of juvenile materials. Nine grains plot close to the Depleted Mantle line and are considered to come from juvenile source materials (Figure 6b). Early Paleozoic zircons from this sample, with crystallization age

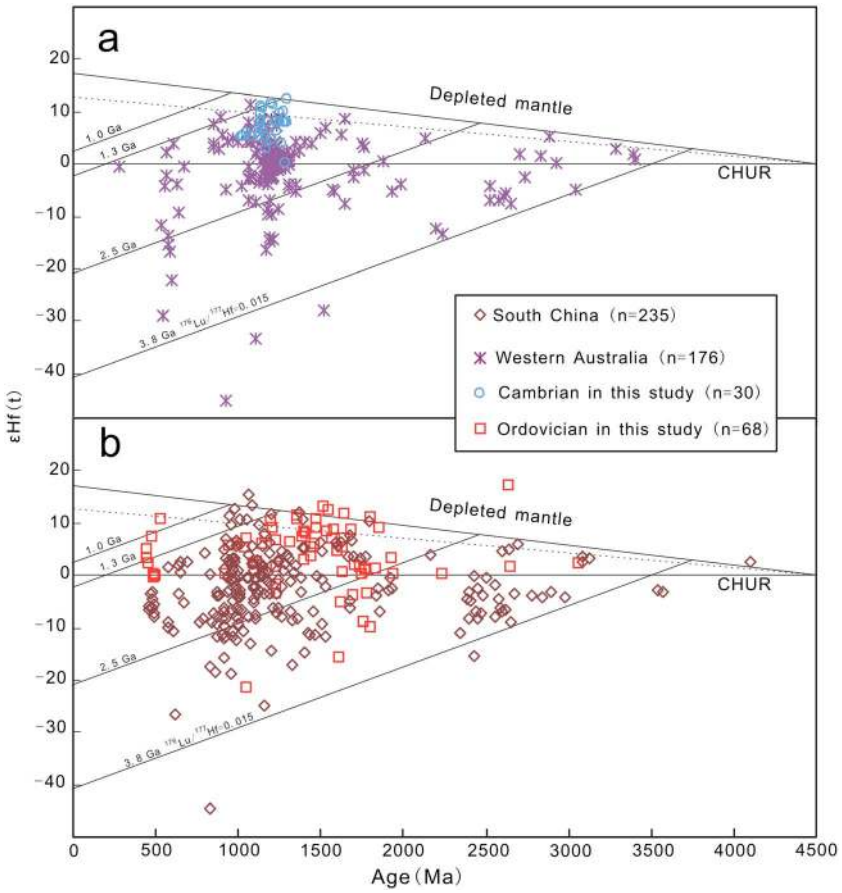


**Figure 6.** Plots of $\varepsilon_{Hf}(t)$ versus U-Pb ages of the detrital zircons from (a) the Cambrian and (b) Ordovician strata in the Sanya Block [this study]. The detrital zircon data from Western Australia (Figure 6a) [*Veever et al*., 2005] and South China (Figure 6b) [*Xu et al*., 2013, 2014] are shown for comparison. CHUR-chondritic uniform reservoir, *n* = total number of analyses. Data plotting above the dashed line are defined as "juvenile": they have $\varepsilon_{Hf} \geq 0.75$, the $\varepsilon_{Hf}$ of the Depleted Mantle [*Belousova et al*., 2010]. The declining parallel lines are two-stage Hf model ages ($T_{DM2}$). Data details are given in Table S2.

of0.5–0.45 Ga, yield generally positive $\varepsilon_{Hf}(t)$ values of −0.1 to 11. Their model ages change from 1.3 Ga to 0.7 Ga, suggesting derivation by reworking of late Mesoproterozoic-Neoproterozoic crust and addition of juvenile materials during the early Paleozoic (0.5–0.45 Ga).

## 6. Discussion and Conclusions

### 6.1. Sources of Detrital Zircons

Analyzed zircons from the Cambrian and Ordovician units at Sanya show distinctive U-Pb and Hf isotopic age spectra and, by inference, distinctive source regions. The zircon age distribution of the Cambrian samples is dominated by late Paleoproterozoic-Mesoproterozoic grains between ~ 1750 Ma and 1000 Ma with a unimodal peak at ~ 1150 Ma. There is only minor Archean to early Paleoproterozoic detritus (sample 11SY-1, Figure 7b). In contrast, zircon ages from the Ordovician sample show a broader age spectrum characterized by a range of late Paleoproterozoic to early Mesoproterozoic ages (1.8–1.4 Ga), along with subordinate late Mesoproterozoic to early Neoproterozoic (1.25–0.9 Ga) ages and a few grains with late Archean ages (Figure 7a). Early Paleozoic zircons are present and yield ages in the range 520 Ma to 450 Ma. Neoproterozoic grains in the range ~ 900 Ma to 600 Ma are absent.

The detrital zircon age population of Cambrian strata at Sanya is distinct from temporally equivalent strata on the mainland of South China and from North India. The Sanya material is characterized by a more unimodal character with a single peak at around 1140 Ma (Figure 7b), whereas the South China mainland and

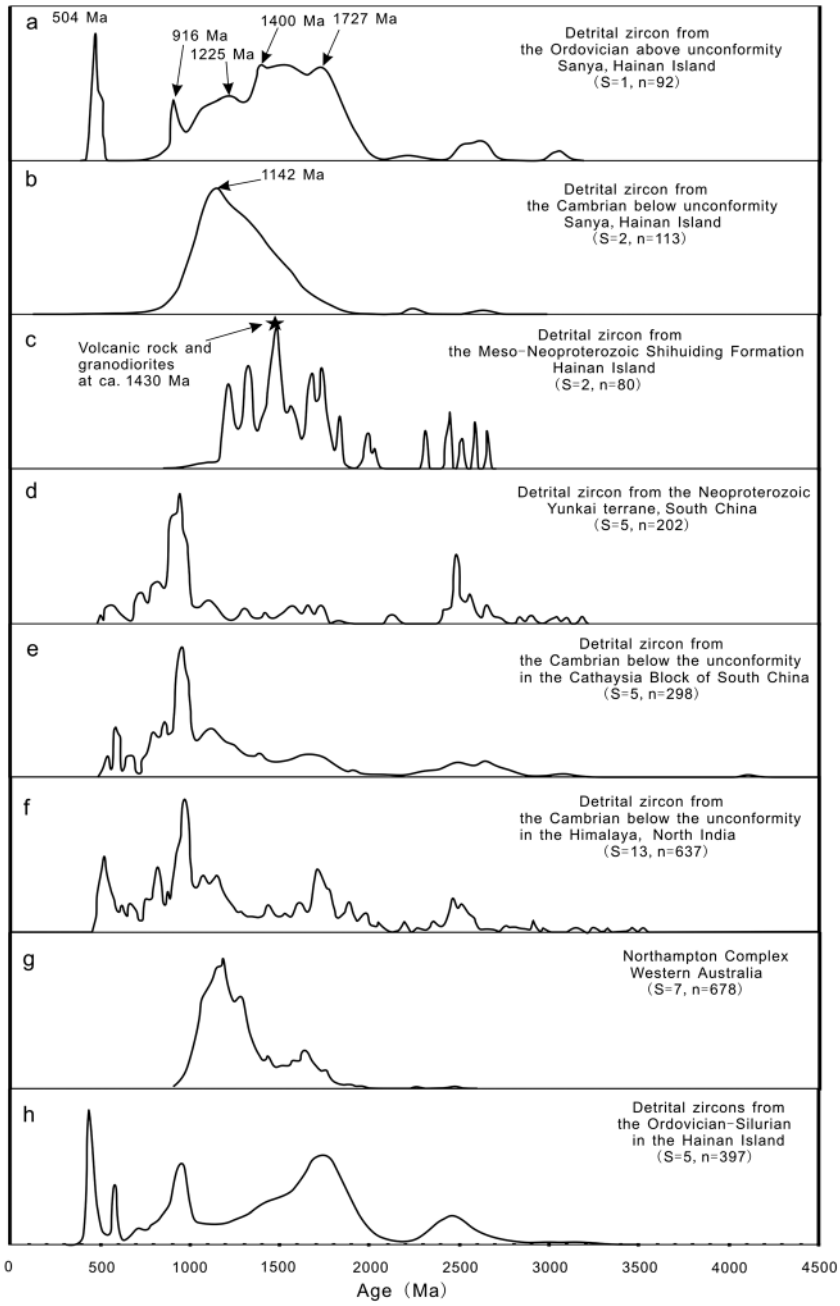


**Figure 7.** Summary of detrital zircon age distributions of samples from (a) the Ordovician strata above the unconformity in the Sanya region [this study], (b) the Cambrian strata below the unconformity in the Sanya region [this study], (c) the basement of Qiongzhong Block [*Li et al*., 2002, 2008], (d) Precambrian basement of the Yunkai domain in the mainland of South China [*Yu et al*., 2008, 2010], (e) the Cambrian strata below the unconformity in the Cathaysia Block of South China [*Xu et al*., 2013, 2014], (f) the Cambrian strata below the unconformity in the Himalaya, North India [*McQuarrie et al*., 2008, 2013; *Myrow et al*., 2009, 2010; *Hughes et al*., 2011; *Long et al*., 2011], (g) the Northampton Complex below the unconformity in Western Australia [*Ksienzyk et al*., 2012], and (h) the Ordovician-Silurian strata in the Hainan Island [*Zhou et al*., 2014]. *s* = number of samples, *n* = total number of analyses. All data based on analyses within 90%–110% of concordance. Ages greater than 1000 Ma calculated using $^{207}Pb/^{206}Pb$ ratios and ages less than 1000 Ma calculated from $^{206}Pb/^{238}U$ ratios. Data details are given in Table S1.

North India strata display a multimodal pattern with a dominant peak at 950 Ma and subordinate peaks at 2500 Ma, 1660 Ma, 1125 Ma, and 580 Ma (Figures 7d–7f) [*Wang et al*., 2010; *Xiang and Shu*, 2010; *Myrow et al*., 2010; *Yao et al*., 2011; *McKenzie et al*., 2011b; *Xu et al*., 2013, 2014; *Yao et al*., 2014; *J. Q. Wang et al*., 2014].

Cambrian strata on the mainland of South China accumulated in marine environments [*Wang et al*., 2010; *Xu et al*., 2013; *Shu et al*., 2014], which together with the absence of middle to late Mesoproterozoic rock units on the mainland, suggests that the bulk of the South China Craton was submerged and could not have acted as a source for sediments in the Sanya Block, Hainan Island.

The age spectrum of the Cambrian quartz sandstones in the Sanya Block and, in particular. the presence of a late Mesoproterozoic age peak at ~ 1150 Ma, is similar to the timing of orogenic events in the Wilkes-Albany-Fraser orogenic belt (Figure 1). It is also similar to sedimentary units derived from this belt such as paragneiss in the Mesoproterozoic Northampton Complex in Western Australia, which forms part of the basement to the Paleozoic to Mesozoic Perth Basin (Figure 7g). The paragneisses were deformed and metamorphosed at 1090–1020 Ma [*Ksienzyk et al*., 2012], which is similar to some of the ages determined for metamorphic grains in the Cambrian samples (Figure 4). Furthermore, the complex is overlain by Ordovician sandstones [*Cawood and Nemchin*, 2000] suggesting it or equivalent successions were likely emergent and subject to erosion in the Cambrian. The Hf isotopic composition of the Cambrian sandstones at Sanya overlaps with that of detrital grains of similar age from the Paleozoic basins of Western Australia (Figure 6a) [*Veever et al*., 2005]. These stratigraphic and chronological relationships are consistent with derivation of the Cambrian sedimentary units at Sanya from a source to the south, within East Gondwana, either the Wilkes-Albany-Fraser belt or metasedimentary successions previously derived from this belt such as the Northampton Complex and/or equivalents.

The broader age spectrum of the Ordovician sample indicates a change in the nature of the source region. The middle to late Mesoproterozoic detritus could have been derived from a similar source to the Cambrian succession or from reworking of the unconformably underlying Cambrian strata. Sources for the late Paleoproterozoic to early Mesoproterozoic detritus include the nearby basement to the Qiongzhong Block, the Baoban and Shilu groups, which contain detrital zircons with a similar age range and are intruded by ~ 1430 Ma granites (Figure 7c) [*Li et al*., 2002, 2008]. Potential sources for the early Neoproterozoic and early Paleozoic detritus within the Ordovician sample occur in South China (Figures 7d and 7e) [*Wang et al*., 2010; *Xiang and Shu*, 2010; *Yao et al*., 2011; *Xu et al*., 2013, 2014; *Yao et al*., 2014; *J. Q. Wang et al*., 2014]. However, early Paleozoic sedimentary units in South China that include material derived from such sources also include middle to late Neoproterozoic detritus, which is absent from the Ordovician sample at Sanya (Figure 7a), suggesting a more restricted source. Furthermore, the early Paleozoic grains from the Ordovician strata have positive $\varepsilon_{Hf}(t)$ values, which contrasts with the negative $\varepsilon_{Hf}(t)$ values of coeval grains preserved in South China Craton (Figure 6b).

The early Neoproterozoic and early Paleozoic zircons within the Ordovician sample display a euhedral, prismatic shape (e.g., 449 Ma grain numbered as 12LHT-2-45 in Figure S2d) suggesting that they are first-cycle detritus from a proximal source. An early Paleozoic arc assemblage is exposed in the center of Hainan Island near Tunchang (Figure 3) [*Xu et al*., 2007, 2008]. These rocks have yielded U-Pb ages in the range 514–442 Ma and were derived from a depleted, primitive mantle arc source [*Xu et al*., 2008]. We consider these rocks a possible source for the zircons of this age (520–450 Ma) in the Sanya sample. The nearest exposed source of early Neoproterozoic rocks is located in the Yunkai region on the mainland [*Wang et al*., 2013b; *Y. J. Wang et al*., 2014]. The full extent of these rocks is unknown due to younger cover, including extensive Mesozoic igneous rocks between the Yunkai and the coastline. Furthermore, paleocurrent data for the Ordovician strata on the mainland indicate derivation from the southeast beyond the current exposed limits of the mainland South China craton [*Wang et al*., 2010; *Shu et al*., 2014; *Xu et al*., 2014]. The prominent early Neoproterozoic (900 Ma) peak in this early Paleozoic strata is generally thought to be derived from an east India source [*Wang et al*., 2010; *Xu et al*., 2013, 2014] and used to constrain the paleogeography of the region. In summary, the Ordovician strata appear to record the input of detritus of relatively local provenance from elsewhere on Hainan Island as well as detritus from farther afield.

### 6.2. Relations to South China and Gondwana Assembly

Comparison of available geological data for the Sanya Block with that for mainland South China, as well as other blocks from northeast Gondwana, provides important constraints on paleogeography and potential

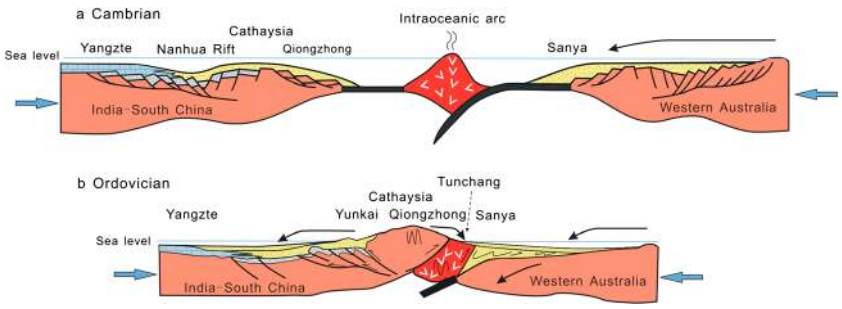


**Figure 8.** Series of sketches showing the amalgamation of South China Craton and Western Australia Craton during the Cambrian-Ordovician period.

timing of assembly of blocks within this segment of Gondwana. Recent work has suggested that the South China Craton was located at the nexus between India, Antarctica, and Australia, along the northern margin of East Gondwana during the Cambrian (Figure 1) [*Cawood et al*., 2013; *Xu et al*., 2013, 2014], and this portion of northeast Gondwana provides a probable source for the Mesoproterozoic detritus. Rock units of suitable age occur in the Wilkes-Albany-Fraser belt between southwest Australia and Antarctica [e.g., *Fitzsimons*, 2000a, 2000b; *Cawood and Korsch*, 2008] and are known to have supplied sediment to the Paleozoic basins to the north [e.g., *Cawood and Nemchin*, 2000; *Veever et al*., 2005].

Provenance data in combination with general geological information suggest that in the Cambrian the Sanya Block on Hainan Island was separated from mainland South China with each receiving detritus from different sources. Data from Sanya suggest that it was linked with the Western Australia Craton and environs and received detritus either directly or recycled from the Wilkes-Albany-Fraser belt, which provided the source for the late Mesoproterozoic grains. The absence of detritus of early Neoproterozoic age in the Cambrian samples suggests that the Sanya Block did not receive detritus from eastern India. In contrast, Cambrian strata on the mainland contain both late Mesoproterozoic and early Neoproterozoic age peaks, which are inferred to be derived from Western Australia and India, respectively [*Cawood et al*., 2013; *Xu et al*., 2013, 2014]. The Ordovician sample in the Sanya Block contains prominent late Paleoproterozoic to early Mesoproterozoic detritus as well as early Paleozoic grains, all of which could have been sourced from the northern part of Hainan Island, within the Qiongzhong Block. This suggests that by the Ordovician the Sanya Block was accreted to the Qiongzhong Block and presumably the rest of South China. The arc affinities of the early Paleozoic igneous rocks in the Tunchang area within the Qiongzhong Block suggest that they may record convergence with the Sanya Block, with the unconformity between the Cambrian and Ordovician strata then corresponding with the time of suturing [*Ding et al*., 2002; *Xu et al*., 2007, 2008]. Once sutured, the Qiongzhong Block supplied detritus into the Sanya Block.

The interpretation of a link between the Sanya Block and Australia is further supported by faunal evidence. Abundant specimens of the morphologically distinctive early middle Cambrian xystriduriid trilobite genera *Xystridura* and *Galahetes* in the Sanya Block mimic their prolific occurrence in similar facies in Australia [*Öpik*, 1975; *Kruse*, 1990]. *Xystridura* is also well known in Antarctica [*Palmer and Gatehouse*, 1972; *Soloviev and Gricurov*, 1979]. These genera are, however, sparse or apparently absent from the well-studied middle Cambrian fauna of South China, with the only report being two stratigraphically younger fragmentary and in our view indeterminate specimens that were questionably referred to *Xystridura* [*Yang et al*., 1993]. The fauna dominated by xystriduriids at Sanya thus strongly and independently support the proposed Australian-Antarctic affinity for these rocks. Interestingly, specimens reliably assigned to these genera do also occur rarely in North China, with *Xystridura* known from Xinjiang [*Xiang and Zhang*, 1985] and *Galahetes* from both Xinjiang [*Xiang and Zhang*, 1985] and western Gansu [*Zhou et al*., 1982].

The contrasting age spectrum of the Cambrian and Ordovician samples at Sanya is consistent with an evolving tectonic regime. The youngest detrital grains in the Cambrian samples are over 300 Ma older than its depositional age, which in combination with facies analysis for the these quartz rich sediments [*Fu et al*., 2007] suggests accumulation in a passive margin setting [cf. *Cawood et al*., 2012]. In contrast, the youngest grains in the Ordovician as well as younger Silurian samples from Hainan Island (Figure. 7h) [*Zhou et al*., 2014] include Paleozoic detritus close to the depositional age suggesting accumulation in a convergent or collisional plate

margin setting [cf. *Cawood et al*., 2012]. This is compatible with the Cambrian to Ordovician convergent plate margin existing along the current southeastern coastline of South China [*Cocks and Torsvik*, 2013], which has been identified on the basis of remnants of accretionary prisms and island arc rock types now forming parts of Japan [*Isozaki et al*., 2010; *Isozaki* 2011], Hainan Island [*Ding et al*., 2002; *Xu et al*., 2007, 2008], and the Song Ma belt [*Findlay*, 1997].

The late Cambrian to early Ordovician age range of the unconformity in the Sanya Block and resultant inferred suturing with the Qiongzhong Block corresponds with timing of orogenic activity extending along the northern margin of Gondwana [*DeCelles et al*., 2000; *Gehrels et al*., 2003; *Chatterjee et al*., 2007; *Yin et al*., 2010a, 2010b; *Myrow et al*., 2010; *Pullen et al*., 2011; *Guynn et al*., 2012] and termed the Bhimphedian Orogeny (530–470 Ma) [*Cawood et al*., 2007]. This also overlaps with final assembly of major cratonic blocks within Gondwana and, in particular, the Kuunga suture [*Fitzsimons*, 2000a; *Boger et al*., 2001; *Meert*, 2003; *Cawood and Buchan*, 2007]. Paleomagnetic records suggest that India and Australia were separated by over 30°of latitude at ~ 750 Ma [e.g., *Torsvik et al*., 2001; *Pisarevsky et al*., 2003; *Zhang et al*., 2013] but were adjacent to each other in the equatorial position by the end Neoproterozoic to early Paleozoic (~ 600–520 Ma) in an assembled Gondwana [e.g., *Powell et al*., 1993; *Powell and Pisarevsky*, 2002]. The middle Cambrian and Silurian paleomagnetic data from South China Craton show that the craton was most probably in an equatorial position and close to Western Australia [*Yang et al*., 2004]. These paleomagnetic constraints are consistent with faunal data that suggest a close link in the early to middle Paleozoic, including the presence of dikelokephalinid trilobites found in both South China and Australia in the Early Ordovician [e.g., *Torsvik and Cocks*, 2009] and Early Devonian fresh water fish in South China, Vietnam, and the Canning Basin of Western Australia [e.g., *Burrett et al*., 1990]. The proposed Cambrian to Ordovician age for closure of the ocean separating the Sanya and Qiongzhong blocks is somewhat younger than the favored latest Neoproterozoic to Cambrian age for collision of India and Australia [e.g., *Meert*, 2003; *Collins and Pisarevsky*, 2005; *Cawood and Buchan*, 2007; *Boger*, 2011] and consistent with the incoming of inferred India-derived detritus into the Ordovician strata of the Sanya Block. Thus, if South China, including the Qiongzhong Block, was linked to northern India and the Sanya Block was tied to Western Australia, these relations suggest that India and Australia were separated in the Cambrian but juxtaposed across the Kuunga suture by the early to mid-Ordovician (Figure 8).

**Acknowledgments**

Data supporting Figures 5 and 7 are available in Table S1 of the supporting information. Data supporting Figure 6 are available in Table S2 of the supporting information. We would like to thank Victor Kovach, three anonymous reviewers, and the Associate Editor for their comments that led to significant improvements in the manuscript. Editor Nathan Niemi is also thanked for his encouragement. Mulong Chen and Xiaowen Zhang from the Bureau of Geology and Mineral Resources of Hainan Province are thanked for their help during fieldwork. Yongsheng Liu and Zhaochu Hu provided help with zircon U-Pb and Hf Isotope analyses. This work was supported by the National Natural Science Foundation of China (grants 41472086 and 41272120), "111" Project (B08030), the fundamental Research Funds for the Central Universities, China University of Geosciences (Wuhan) (CUG2012019240 and CUG2013019137). The first author also acknowledges China Scholarship Council (grant 201208420001) for supporting his research in the University of St. Andrews.

## References

Ali, J. R., H. M. C. Cheung, J. C. Aitchison, and Y. Sun (2013), Palaeomagnetic re-investigation of Early Permian rift basalts from the Baoshan Block, SW China: Constraints on the site-of-origin of the Gondwana-derived eastern Cimmerian terranes, *Geophys. J. Int.*, *193*, 650–663.

Belousova, E. A., Y. A. Kostitsyn, G. C. Begg, W. L. Griffin, S. Y. O'Reilly, and N. J. Pearson (2010), The growth of the continental crust: Constraints from zircon Hf-isotope data, *Lithos*, *119*, 457–466.

Blichert-Toft, J. (2008), The Hf isotopic composition of zircon reference material 91500, *Chem. Geol.*, *253*(3–4), 252–257.

Blichert-Toft, J., and F. Albarede (1997), The Lu-Hf isotope geochemistry of chondrites and the evolution of the mantle-crust system, *Earth Planet. Sci. Lett.*, *148*, 243–258.

Boger, S. D. (2011), Antarctica—Before and after Gondwana, *Gondwana Res.*, *19*, 335–371.

Boger, S. D., and J. M. Miller (2004), Terminal suturing of Gondwana and the onset of the Ross–Delamerian Orogeny: The cause and effect of an Early Cambrian reconfiguration of plate motions, *Earth Planet. Sci. Lett.*, *219*, 35–48.

Boger, S. D., C. J. L. Wilson, and C. M. Fanning (2001), Early Paleozoic tectonism within the East Antarctic craton: The final suture between east and west Gondwana?, *Geology*, *29*, 463–466.

Bureau of Geology and Mineral Resources of Guangdong Province (BGMRGP) (1988), *Regional Geology of the Guangdong Province* [in Chinese with English abstract], Geo. Mem. Ser. 1., vol. 9, pp. 941, Geol. Publ. House, Beijing.

Burrett, C., J. Long, and B. Stait (1990), Early-Middle Palaeozoic biogeography of Asian terranes derived from Gondwana, in *Palaeozoic Palaeogeography and Biogeography*, edited by W. S. McKerrow and C. R. Scotese, *Mem. Geol. Soc. London*, *12*, 163–174, doi:10.1144/GSL.MEM.1990.012.01.14.

Cawood, P. A., and C. Buchan (2007), Linking accretionary orogenesis with supercontinent assembly, *Earth Sci. Rev.*, *82*, 217–256.

Cawood, P. A., and R. J. Korsch (2008), Assembling Australia: Proterozoic building of a continent, *Precambrian Res.*, *166*, 1–38.

Cawood, P. A., and A. A. Nemchin (2000), Provenance record of a rift basin: U/Pb ages of detrital zircons from the Perth Basin, Western Australia, *Sediment. Geol.*, *134*, 209–234.

Cawood, P. A., M. R. W. Johnson, and A. A. Nemchin (2007), Early Palaeozoic orogenesis along the Indian margin of Gondwana: Tectonic response to Gondwana assembly, *Earth Planet. Sci. Lett.*, *255*, 70–84.

Cawood, P. A., C. J. Hawkesworth, and B. Dhuime (2012), Detrital zircon record and tectonic setting, *Geology*, *40*(10), 875–878.

Cawood, P. A., Y. J. Wang, Y. J. Xu, and G. C. Zhao (2013), Locating South China in Rodinia and Gondwana: A fragment of Greater India Lithosphere?, *Geology*, *41*, 903–906.

Chatterjee, N., A. C. Mazumdar, A. Bhattacharya, and R. R. Saikia (2007), Mesoproterozoic granulites of the Shillong-Meghalaya Plateau: Evidence of westward continuation of the Prydz Bay Pan-African suture into Northeastern India, *Precambrian Res.*, *152*, 1–26.

Cocks, L. R. M., and T. H. Torsvik (2013), The dynamic evolution of the Palaeozoic geography of eastern Asia, *Earth Sci. Rev.*, *117*, 40–79.

Collins, A. S. (2003), Structure and age of the northern Leeuwin Complex, Western Australia: Constraints from field mapping and U–Pb analysis, *Aust. J. Earth Sci.*, *50*, 585–599.

Collins, A. S., and S. A. Pisarevsky (2005), Amalgamating eastern Gondwana: The evolution of the Circum-Indian Orogens, *Earth Sci. Rev.*, *71*, 229–270.
DeCelles, P. G., G. E. Gehrels, J. Quade, B. LaReau, and M. Spurlin (2000), Tectonic implications of U-Pb zircon ages of the Himalayan orogenic belt in Nepal, *Science*, *288*, 497–499.
Ding, S. J., C. H. Xu, W. G. Long, Z. Y. Zhou, and Z. T. Liao (2002), Tectonic attribute and geochronology of metavolcanic rocks, Tunchang, Hainan Island, *Acta Petrol. Sin.*, *18*, 83–90.
Elhlou, S., E. Belousova, W. L. Griffin, N. J. Pearson, and S. Y. O'Reilly (2006), Trace element and isotopic composition of GJ-red zircon standard by laser ablation, *Geochim. Cosmochim. Acta*, *70*, A158.
Findlay, R. H. (1997), The Song Ma Anticinorium, northern Vietnam: The structure of an allochthonous terrane containing an early Palaeozoic island arc sequence, *J. Asian Earth Sci.*, *15*, 453–464.
Fitzsimons, I. C. W. (2000a), A review of tectonic events in the East Antarctic Shield, and their implications for Gondwana and earlier supercontinents, *J. African Earth Sci.*, *31*, 3–23.
Fitzsimons, I. C. W. (2000b), Grenville aged basement provinces in East Antarctica: Evidence for three separate collisional orogens, *Geology*, *28*, 879–882.
Fitzsimons, I. C. W. (2003), Proterozoic basement provinces of southwestern Australia, and their correlation with Antarctica, In *Proterozoic East Gondwana: Supercontinent Assembly and Breakup*, edited by Y. Yoshida, B. F. Windley, and S. Dasgupta, *Geol. Soc. London Spec. Publ.*, *206*, 93–130.
Fu, G. X., Li, M., and Zeng, W. J. (2007), Geology of Hainan Province, in *Geological Atlas of China*, edited by L. F. Ma, pp. 269–275, Geol. Publ. House, Beijing.
Gehrels, G., et al. (2011), Detrital zircon geochronology of pre-Tertiary strata in the Tibetan-Himalayan orogen, *Tectonics*, *30*, TC5016, doi:10.1029/2011TC002868.
Gehrels, G. E., P. G. DeCelles, A. Martin, T. P. Ojha, G. Pinhassi, and B. N. Upreti (2003), Initiation of the Himalayan Orogen as an early Paleozoic thin-skinned thrust belt, *Geol. Soc. Am. Today*, *13*, 4–9.
Gehrels, G. E., P. G. DeCelles, T. P. Ojha, and B. N. Upreti (2006a), Geologic and U–Th–Pb geochronologic evidence for early Paleozoic tectonism in the Kathmandu thrust sheet, central Nepal Himalaya, *Geol. Soc. Am. Bull.*, *118*, 185–198.
Gehrels, G. E., P. G. DeCelles, T. P. Ojha, and B. N. Upreti (2006b), Geologic and U–Pb geochronologic evidence for early Paleozoic tectonism in the Dadeldhura thrust sheet, far-west Nepal Himalaya, *J. Asian Earth Sci.*, *28*, 385–408.
Griffin, W. L., X. Wang, S. E. Jackson, N. J. Pearson, S. Y. O'Reilly, X. Xu, and X. Zhou (2002), Zircon chemistry and magma mixing, SE China: In situ analysis of Hf isotopes, Tonglu and Pingtan igneous complexes, *Lithos*, *61*(3), 237–269.
Grunow, A., R. Hanson, and T. Wilson (1996), Were aspects of Pan-African deformation linked to Iapetus opening?, *Geology*, *24*, 1063–1066.
Guynn, J., P. Kapp, G. E. Gehrels, and L. Ding (2012), U–Pb geochronology of basement rocks in central Tibet and paleogeographic implications, *J. Asian Earth Sci.*, *43*, 23–50.
Hofmann, M., U. Linnemann, V. Rai, S. Becker, A. Gärtner, and A. Sagawe (2011), The India and South China cratons at the margin of Rodinia—Synchronous Neoproterozoic magmatism revealed by LA-ICP-MS zircon analyses, *Lithos*, *123*, 176–187.
Hu, Z. C., et al. (2012), Improved in situ Hf isotope ratio analysis of zircon using newly designed X skimmer cone and jet sample cone in combination with the addition of nitrogen by laser ablation multiple collector ICP-MS, *J. Anal. At. Spectrom.*, *27*, 1391–1399, doi:10.1039/C2JA30078H.
Hughes, N. C., S. C. Peng, O. N. Bhargava, A. D. Ahulwalia, S. Walia, P. M. Myrow, and S. K. Parcha (2005), The Cambrian biostratigraphy of the Tal Group, Lesser Himalaya, India, and early Tsanglangpuan (late early Cambrian) trilobites from the Nigali Dhar syncline, *Geol. Mag.*, *142*, 57–80.
Hughes, N. C., P. M. Myrow, R. N. McKenzie, D. A. T. Harper, O. N. Nhargava, S. K. Tangri, K. S. Ghalley, and C. M. Fanning (2011), Cambrian rocks and faunas of the Wachi La, Black Mountains, Bhutan, *Geol. Mag.*, *148*(3), 351–379.
Isozaki, Y. (2011), Ordovician rocks in Japan, in *Ordovician of the World*, edited by J. C. Gutierrez-Marco, I. Rabano, and D. Garcia-Bollido, pp. 251–252, Instituto Geologico y Minero de Espana, Madrid.
Isozaki, Y., K. Aoki, T. Nakama, and S. Yanai (2010), New insight into a subduction-related orogen: A reappraisal of the geotectonic framwork and evolution of the Japanese Islands, *Gondwana Res.*, *18*, 82–105.
Jacobs, J., C. M. Fanning, F. Henjes-Kunst, M. Olesch, and H. Paech (1998), Continuation of the Mozambique Belt into East Antarctica: Grenville-age metamorphism and polyphase Pan-African high-grade events in central Dronning Maud Land, *J. Geol.*, *106*, 385–406.
Jiang, G., L. E. Sohl, and N. Christie-Blick (2003), Neoproterozoic stratigraphic comparison of the Lesser Himalaya (India) and Yangtze block (South China): Paleogeographic implications, *Geology*, *31*, 917–920.
Kruse, P. D. (1990), Cambrian palaeontology of the Daly Basin, Northern Territory Geological Survey Report, *7*, 1–58.
Ksienzyk, A. K., J. Jacobs, S. D. Boger, J. Kosler, K. N. Sircombe, and K. N. Whitehouse (2012), U–Pb ages of metamorphic monazite and detrital zircon from the Northampton Complex: Evidence of two orogenic cycles in Western Australia, *Precambrian Res.*, *198-199*, 37–50.
Li, T. R., and J. B. Jago (1993), Xystridura and other early middle Cambrian trilobites from Yaxian, Hainan Province, China, *Trans. R. Soc. South Aust.*, *117*, 141–152.
Li, X. H., Z. X. Li, W. X. Li, and Y. J. Wang (2006), Initiation of the Indosinian Orogeny in South China: Evidence for a Permian magmatic arc in the Hainan Island, *J. Geol.*, *114*, 341–353.
Li, Z. X., X. H. Li, H. W. Zhou, and P. D. Kinny (2002), Grenvillian continental collision in South China: New SHRIMP U–Pb zircon results and implications for the configuration of Rodinia, *Geology*, *30*, 163–166.
Li, Z. X., X. H. Li, W. X. Li, and S. J. Ding (2008), Was Cathaysia part of Proterozoic Laurentia? New data from Hainan Island, South China, *Terra Nova*, *20*, 154–164.
Liu, X. C., B. M. Jahn, Y. Zhao, G. C. Zhao, and X. H. Liu (2007a), Geochemistry and geochronology of high-grade rocks from the Grove Mountains, Eastern Antarctica: Evidence for a Neoproterozoic basement metamorphosed during a single Cambrian tectonic cycle, *Precambrian Res.*, *158*, 93–118.
Liu, X. C., Y. Zhao, G. C. Zhao, P. Jian, and G. Xu (2007b), Petrology and geochronology of granulites from the McKaskle Hills, Eastern Amery Ice Shelf, Antarctica, and implications for the evolution of the Prydz Belt, *J. Petrol.*, *48*, 1443–1470.
Liu, Y. S., S. Gao, Z. C. Hu, C. Gao, K. Zong, and D. Wang (2010), Continental and oceanic crust recycling-induced melt-peridotite interactions in the Trans-North China Orogen: U-Pb dating, Hf isotopes and trace elements in zircons of mantle xenoliths, *J. Petrol.*, *51*, 537–571.
Long, S., N. McQuarrie, T. Tobgay, C. Rose, G. Gehrels, and D. Grujic (2011), Tectonostratigraphy of the Lesser Himalaya of Bhutan: Implications for the along-strike stratigraphic continuity of the northern Indian margin, *Geol. Soc. Am. Bull.*, *123*, 1406–1426.
Ludwig, K. R. (2003), User's manual for Isoplot 3.00: A geochronological toolkit for Microsoft Excel Special Publication 4, Berkeley Geochronology Center.
Ma, D., X. Huang, Z. Z. Chen, Z. Xiao, W. Zhang, and S. Zhong (1997), New advanced in the study of the Baoban Group in Hainan Province, *Reg. Geol. China*, *16*(2), 130–192.

McKenzie, N. R., N. C. Hughes, P. M. Myrow, D. K. Choi, and T. Park (2011a), Trilobites and zircons link north China with the eastern Himalaya during the Cambrian, *Geology*, *39*, 591–594.
McKenzie, N. R., N. C. Hughes, P. M. Myrow, S. H. Xiao, and M. Sharma (2011b), Correlation of Precambrian–Cambrian sedimentary successions across northern India and the utility of isotopic signatures of Himalayan lithotectonic zones, *Earth Planet. Sci. Lett.*, *312*, 471–483.
McQuarrie, N., D. Robinson, S. Long, T. Tobgay, D. Grujic, G. Gehrels, and M. Ducea (2008), Preliminary stratigraphic and structural architecture of Bhutan: Implications for the along-strike architecture of the Himalayan system, *Earth Planet. Sci. Lett.*, *272*, 105–117.
McQuarrie, N., S. P. Long, T. Tobgay, J. N. Nesbit, G. Gehrels, and M. N. Ducea (2013), Documenting basin scale, geometry and provenance through detrital geochemical data: Lessons from the Neoproterozoic to Ordovician Lesser, Greater, and Tethyan Himalayan strata of Bhutan, *Gondwana Res.*, *23*, 1491–1510.
Meert, J. G. (2003), A synopsis of events related to the assembly of eastern Gondwana, *Tectonophysics*, *362*, 1–40.
Meert, J. G., and B. S. Lieberman (2008), The Neoproterozoic assembly of Gondwana and its relationship to the Ediacaran–Cambrian radiation, *Gondwana Res.*, *14*, 5–21.
Meert, J. G., and R. Van der Voo (1997), The assembly of Gondwana 800–500 Ma, *J. Geodyn.*, *23*, 223–235.
Meert, J. G., R. Van der Voo, and S. Ayub (1995), Paleomagnetic investigation of the Neoproterozioic Gagwe lavas and Mbozi Complex, Tanzania and the assembly of Gondwana, *Precambrian Res.*, *74*, 225–244.
Metcalfe, I. (1996), Gondwanaland dispersion, Asian accretion and evolution of eastern Tethys, *Aust. J. Earth Sci.*, *43*, 605–623.
Metcalfe, I. (2006), Palaeozoic and Mesozoic tectonic evolution and palaeogeography of East Asian crustal fragments: The Korean Peninsula in context, *Gondwana Res.*, *9*, 24–46.
Metcalfe, I. (2013), Gondwana dispersion and Asian accretion: Tectonic and palaeogeographic evolution of eastern Tethys, *J. Asian Earth Sci.*, *66*, 1–33.
Myrow, P. M., N. C. Hughes, M. P. Searle, C. M. Fanning, S. C. Peng, and S. K. Parcha (2009), Stratigraphic correlation of Cambrian–Ordovician deposits along the Himalaya: Implications for the age and nature of rocks in the Mount Everest region, *Geol. Soc. Am. Bull.*, *120*, 323–332.
Myrow, P. M., N. C. Hughes, J. W. Goodge, C. M. Fanning, I. S. Williams, S. C. Peng, O. N. Bhargava, S. K. Parcha, and K. R. Pogue (2010), Extraordinary transport and mixing of sediment across Himalayan central Gondwana during the Cambrian–Ordovician, *Geol. Soc. Am. Bull.*, *122*, 1660–1670.
Öpik, A. A. (1975), Templetonian and Ordian xystridurid trilobites of Australia, *Bur. Miner. Resour., Geol. Geophys., Bull.*, *121*, 1–84.
Palmer, A. R., and C. G. Gatehouse (1972), Early and Middle Cambrian trilobites from Antarctica United States Geological Survey Professional Papers 456-D, pp. 1–36.
Pisarevsky, S.A., M. T. D. Wingate, C. M. Powell, S. Johnson, and D. A. D. Evans (2003), Models of Rodina assembly and fragmentation, in *Proterozoic East Gondwana: Supercontinent Assembly and Break-Up*, edited by M. Yoshida, B. F. Windley, and S. Dasgupta, *Geol. Soc. London Spec. Publ.*, *206*, 35–55.
Powell, C. M., and S. A. Pisarevsky (2002), Late Neoproterozoic assembly of East Gondwana, *Geology*, *30*, 3–6.
Powell, C. M. A., Z. X. Li, M. W. McElhinny, J. G. Meert, and J. K. Park (1993), Palaeomagnetic constraints of the Neoproterozoic breakup of Rodinia and the Cambrian formation of Gondwana, *Geology*, *21*, 889–892.
Pullen, A., P. Kapp, G. E. Gehrels, L. Ding, and Q. H. Zhang (2011), Metamorphic rocks in central Tibet: Lateral variations and implications for crustal structure, *Geol. Soc. Am. Bull.*, *123*, 585–600.
Shu, L., B. M. Jahn, J. Charvet, M. Santosh, B. Wang, X. S. Xu, and S. Y. Jiang (2014), Early Paleozoic depositional environment and intraplate tectono-magmatism in the Cathaysia Block (South China): Evidence form stratigraphic, structural, geochemical and geochronological investigations, *Am. J. Sci.*, *314*, 154–186.
Smit, M. A., B. R. Hacker, and J. Lee (2014), Tibetan garnet records early Eocene initiation of thickening in the Himalaya, *Geology*, *42*, 591–594.
Soderlund, U., P. J. Patchett, J. D. Vervoort, and C. Isachsen (2004), The $^{176}$Lu decay constant determined by Lu-Hf and U-Pb isotope systematics of Precambrian mafic intrusions, *Earth Planet. Sci. Lett.*, *219*, 311–324.
Soloviev, I. A., and G. E. Gricurov (1979), New evidence on distribution of Cambrian trilobites in Argentina and Shackleton Ranges in the Antarctic/Antarktika: The Committee Reports, pp. 54–73, Academy of Sciences of the USSR, Soviet Committee on Antarctic Research, Moscow.
Sun, Y. C. (1963), On the occurrence of Xystridura fauna from Middle Cambrian of Hainan Island and its significance, *Acta Paleontolog Sin.*, *11*, 608–611.
Torsvik, T. H., and L. R. M. Cocks (2009), The Lower Palaeozoic palaeogeographical evolution of the northeastern and eastern peri-Gondwanan margin from Turkey to New Zealand, *Geol. Soc. London Spec. Publ.*, *325*, 3–21.
Torsvik, T. H., L. M. Carter, L. D. Ashwal, S. K. Bhushan, M. K. Pandit, and B. Jamtveit (2001), Rodinia refined or obscured: Palaeomagnetism of the Malani igneous suite (NW India), *Precambrian Res.*, *108*, 319–333.
Usuki, T., C. Y. Lan, K. L. Wang, and H. Y. Chiu (2013), Linking the Indochina block and Gondwana during the Early Paleozoic: Evidence from U–Pb ages and Hf isotopes of detrital zircons, *Tectonophysics*, *586*, 145–159.
Veever, J. J., A. Saeed, E. A. Belousova, and W. L. Griffin (2005), U–Pb ages and source composition by Hf-isotope and trace-element analysis of detrital zircons in Permian sandstone and modern sand from southwestern Australia and a review of the paleogeographical and denudational history of the Yilgarn Craton, *Earth Sci. Rev.*, *68*, 245–279.
Vervoort, J. D., and J. Blichert-Toft (1999), Evolution of the depleted mantle: Hf isotope evidence from juvenile rocks through time, *Geochim. Cosmochim. Acta*, *63*(3–4), 533–556.
Wang, J. Q., L. S. Shu, M. Santosh, and Z. Q. Xu (2014), The Pre-Mesozoic crustal evolution of the Cathaysia Block, South China: Insights from geological investigation, zircon U–Pb geochronology, Hf isotope and REE geochemistry from the Wugongshan complex, *Gondwana Res.*, doi:10.1016/j.gr.2014.03.008.
Wang, X. F., D. Q. Ma, and D. Jiang (1991), *Geology of Hainan Island: The 3rd, The Structural Geology* [in Chinese], pp. 140, Geol. Pub. House, Beijing.
Wang, Y. J., W. M. Fan, G. C. Zhao, S. C. Ji, and T. P. Peng (2007), Zircon U–Pb geochronology of gneissic rocks in the Yunkai massif and its implications on the Caledonian event in the South China Block, *Gondwana Res.*, *12*, 404–416.
Wang, Y. J., F. F. Zhang, W. M. Fan, G. W. Zhang, S. Y. Chen, P. A. Cawood, and A. M. Zhang (2010), Tectonic setting of the South China Block in the early Paleozoic: Resolving intracontinental and ocean closure models from detrital zircon U-Pb geochronology, *Tectonics*, *29*, TC6020, doi:10.1029/2010TC002750.
Wang, Y. J., X. W. Xing, P. A. Cawood, S. C. Lai, X. P. Xia, W. M. Fan, H. C. Liu, and F. F. Zhang (2013a), Petrogenesis of early Paleozoic peraluminous granite in the Sibumasu Block of SW Yunnan and diachronous accretionary orogenesis along the northern margin of Gondwana, *Lithos*, *182–183*, 67–85.
Wang, Y. J., A. M. Zhang, P. A. Cawood, Y. Z. Zhang, W. M. Fan, and G. W. Zhang (2013b), Geochronological, geochemical and Nd-Hf-Os isotopic fingerprinting of an early Neoproterozoic arc-back-arc system in South China and its accretionary assembly along the margin of Rodinia, *Precambrian Res.*, *231*, 343–371.
Wang, Y. J., Y. Z. Zhang, W. M. Fan, H. Y. Geng, H. P. Zou, and X. W. Bi (2014), Early Neoproterozoic accretionary assemblage in the Cathaysia Block: Geochronological, Lu–Hf isotopic and geochemical evidence from granitoid gneisses, *Precambrian Res.*, *249*, 144–161.

Xia, B., K. Shi, Z. Fang, and J. Yu (1991), The late Paleozoic rifting in Hainan Island, China, *Acta Geol. Sin.*, *65*, 103–115.
Xiang, L., and L. S. Shu (2010), Pre-Devonian tectonic evolution of the eastern South China Block: Geochronological evidence from detrital zircons, *Sci. China Earth Sci.*, *53*(10), 1427–1444, doi:10.1007/s11430-010-4061-5.
Xiang, L., and T. Zhang (1985), *Stratigraphy and Trilobite Faunas of the Cambrian in the Western Part of Northern Tianshan, Xinjiang*, pp. 243, Geol. Pub. House, Beijing.
Xie, C. F., J. C. Zhu, S. J. Ding, Y. M. Zhang, M. L. Chen, Y. R. Fu, T. A. Fu, and Z. H. Li (2006), Age and petrogenesis of the Jianfengling granite and its relationship to metallogenesis of the Baolun gold deposit, Hainan Island, *Acta Petrol. Sin.*, *22*, 2493–2508.
Xu, D. R., B. Xia, P. C. Li, G. H. Chen, C. Ma, and Y. Q. Zhang (2007), Protolith natures and U-Pb sensitive high mass-resolution ion microprobe (SHRIMP) zircon ages of the metabasites in Hainan Island, South China: Implications for geodynamic evolution since the late Precambrian, *Isl Arch.*, *16*, 575–597.
Xu, D. R., B. Xia, N. Bakun-Czubarow, R. Bachlinski, P. Li, and T. Chen (2008), Geochemistry and Sr-Nd isotope systematics of metabasites in the Tunchang area, Hainan Island, South China: Implications for petrogenesis and tectonic setting, *Miner. Petrol.*, *92*, 361–391.
Xu, Y. J., P. A. Cawood, Y. S. Du, L. S. Hu, W. C. Yu, Y. H. Zhu, and W. C. Li (2013), Linking South China to northern Australia and India on the margin of Gondwana: Constraints from detrital zircon U-Pb and Hf isotopes in Cambrian strata, *Tectonics*, *32*, 1547–1558, doi:10.1002/tect.20099.
Xu, Y. J., P. A. Cawood, Y. S. Du, H. W. Huang, and X. Y. Wang (2014), Early Paleozoic orogenesis along Gondwana's northern margin constrained by provenance data from South China, *Tectonophysics*, doi:10.1016/j.tecto.2014.08.022.
Yang, J., S. Yu, G. Liu, N. Su, M. He, J. Shang, H. Zhang, H. Zhu, Y. Li, and G. Yan (1993), *Cambrian Stratigraphy, Lithofacies, Palaeogeography and Trilobite Faunas of the East Qingling-Dabashan Mountains*, pp. 246, The Press of the China Univ. of Geosciences, Wuhan, China.
Yang, S., Z. Yu, L. Guo, and Y. Shi (1989), The division and palaeomagnetism of the Hainan Island and plate tectonic significance, *J. Nanjing Univ. (Earth Sci. Ed.)*, *1*, 38–46.
Yang, Z., Z. Sun, T. Yang, and J. Pei (2004), A long connection (750–380 Ma) between South China and Australia: Paleomagnetic constraints, *Earth Planet. Sci. Lett.*, *220*, 423–434.
Yao, H. Z., Z. X. Huang, C. F. Xie, and C. M. Zhang (1999), The Cambrian lithostratigraphical sequence and sedimentary facies of Wanning Area, Hainan Island, *J. Stratigr.*, *23*(4), 270–276.
Yao, J. L., L. S. Shu, and M. Santosh (2011), Detrital zircon U–Pb geochronology Hf-isotopes and geochemistry—New clues for the Precambrian crustal evolution of Cathaysia Block, South China, *Gondwana Res.*, *20*, 553–567.
Yao, W. H., Z. X. Li, W. X. Li, X. H. Li, and J. H. Yang (2014), From Rodinia to Gondwanaland: A tale of detrital zircons provenance analyses from the southern Nanhua Basin, South China, *Am. J. Sci.*, *314*, 278–313.
Yin, A. (2006), Cenozoic tectonic evolution of the Himalayan orogen as constrained by along-strike variations of structural geometry, exhumation history, and foreland sedimentation, *Earth Sci. Rev.*, *76*, 1–131.
Yin, A., C. S. Dubey, A. A. G. Webb, T. K. Kelty, M. Grove, G. E. Gehrels, and W. P. Burgess (2010a), Geologic correlation of the Himalayan orogen and Indian craton: Part 1. Structural geology, U–Pb zircon geochronology, and tectonic evolution of the Shillong Plateau and its neighboring regions in NE India, *Geol. Soc. Am. Bull.*, *122*, 336–359.
Yin, A., C. S. Dubey, T. K. Kelty, A. A. G. Webb, T. M. Harrison, C. Y. Chou, and J. Celerier (2010b), Geologic correlation of the Himalayan orogen and Indian craton: Part 2. Structural geology, geochronology, and tectonic evolution of the Eastern Himalaya, *Geol. Soc. Am. Bull.*, *122*, 360–395.
Yu, J. H., S. Y. O'Reilly, L. J. Wang, W. L. Griffin, M. Zhang, R. C. Wang, S. Y. Jiang, and L. S. Shu (2008), Where was south China in the Rodinia supercontinent? Evidence from U–Pb geochronology and Hf isotopes of detrital zircons, *Precambrian Res.*, *164*, 1–15.
Yu, J. H., S. Y. O'Reilly, L. . J. Wang, W. L. Griffin, M. F. Zhou, M. Zhang, and L. S. Shu (2010), Components and episodic growth of Precambrian crust in the Cathaysia Block, South China: Evidence from U–Pb ages and Hf isotopes of zircons in Neoproterozoic sediments, *Precambrian Res.*, *181*, 97–114.
Zeng, Q. L., C. L. Yuan, Z. M. Guo, and J. M. Lin (1992), *Fundamental Geological Investigation of Sanya, Hainan Island* [in Chinese with English abstract], pp. 174, The Press of the China Univ. of Geosciences, Wuhan, China.
Zhang, R. J., and Z. W. Jiang (1998), The discovery of early Cambrian microfossils from Wanning County, Hainan Island and its significances, *Acta Palaeontol. Sin.*, *37*(2), 235–244.
Zhang, S., D. A. D. Evans, H. Li, H. Wu, G. Jiang, J. Dong, Q. Zhao, T. D. Raub, and T. Yang (2013), Paleomagnetism of the late Cryogenian Nantuo Formation and paleogeographic implications for the South China Block, *J. Asian Earth Sci.*, *72*, 164–177.
Zhao, G., and P. Cawood (1999), Tectonothermal evolution of the Mayuan assemblage in the Cathaysia block: Implications for neoproterozoic collision-related assembly of the South China Craton, *Am. J. Sci.*, *299*, 309–339.
Zhao, G., and P. Cawood (2012), Precambrian Geology of China, *Precambrian Res.*, *222-223*, 13–54.
Zhao, G. C., and J. H. Guo (2012), Precambrian Geology of China: Preface, *Precambrian Res.*, *222-223*, 1–12.
Zhao, G. C., M. Sun, and S. A. Wilde (2002), Did South America and West Africa marry and divorce or was it a long-lasting relationship?, *Gondwana Res.*, *5*, 591–596.
Zhao, J. H., M. F. Zhou, D. P. Yan, J. P. Zheng, and J. W. Li (2011), Reappraisal of the ages of Neoproterozoic strata in South China: No connection with the Grenvillian orogeny, *Geology*, *39*, 299–302.
Zhao, Z., P. D. Bons, G. Wang, Y. Liu, and Y. Zheng (2014), Origin and pre-Cenozoic evolution of the south Qiangtang basement Central Tibet, *Tectonophysics*, doi:10.1016/j.tecto.2014.03.016.
Zhou, M. F., D. P. Yan, A. K. Kennedy, Y. Q. Li, and J. Ding (2002), SHRIMP U-Pb zircon geochronological and geochemical evidence for Neoproterozoic arc magmatism along the western margin of the Yangtze block, South China, *Earth Planet. Sci. Lett.*, *196*, 51–67.
Zhou, Y., X. Liang, X. Liang, Y. Jiang, C. Wang, J. Fu, and T. Shao (2014), U–Pb geochronology and Hf-isotopes on detrital zircons of Lower Paleozoic strata from Hainan Island: New clues for the early crustal evolution of southeastern South China, *Gondwana Res*, doi:10.1016/j.gr.2014.01.015.
Zhou, Z., J. Li, and X. Qu (1982), Trilobita, in *Paleontological Atlas of Northwest China, Shanxi-Gansu-Ningxia Volume. Part 1: Precambrian and Early Palaeozoic*, pp. 215—294, Geol. Pub. House, Beijing.
Zhu, D. C., Z. D. Zhao, Y. L. Niu, Y. Dilek and X. X. Mo (2011), Lhasa terrane in southern Tibet came from Australia, *Geology*, *39*(8), 727=730.
Zhu, Z. L., and T. R. Lin (1978), Some Middle Cambrian trilobites from Yaxian, Hainan Island, *Acta Palaeontol. Sin.* , *17*, 439–443.